NATIONAL AERONAUTICS AND SPACE ADMINISTRATION

Technical Memorandum 33-745

Scintillation Estimates for a Jupiter Entry Probe—Phase I

R. Woo
F. C. Yang

JET PROPULSION LABORATORY
CALIFORNIA INSTITUTE OF TECHNOLOGY
PASADENA, CALIFORNIA

November 1, 1975

Preface

The work described in this report was carried out by the Telecommunications Division of the Jet Propulsion Laboratory, California Institute of Technology, for the NASA Ames Research Center by agreement with the National Aeronautics and Space Administration.

CONTENTS

Abstract

In this report a model of the electron density irregularities in the Jovian ionosphere is constructed based on a preliminary interpretation of the Pioneer 10 Jovian ionospheric scintillations. The ionospheric irregularities exist over an altitude range of 3000 km. The structure constant c_n of refractive index fluctuations is 5×10^{-9} $m^{-1/3}$ and is constant throughout this altitude range. The spatial wavenumber spectrum of the electron density irregularities follows the Kolmogorov spectrum and the outer scale size is greater than 6 km.

Estimates of scintillation for a Jovian entry probe based on this model indicate that it is small at S-band but could be substantial at 400 MHz. The temporal frequency spectrum of the log-amplitude fluctuations is less than 1 Hz and is consequently rather narrow.

I. Introduction

The objective of this study is to analyze the scintillation of the radio signals received from Pioneers 10 and 11 during radio occultation by the atmosphere of Jupiter and to estimate from these results the scintillation of the signal from a direct entry probe. The study is therefore similar in principle to that carried out for the Pioneer Venus Multiprobe mission based on the Mariner 5 radio occultation data (Refs. 1 and 2). Four steps are necessary to achieve this. First, the radio occultation data is processed and the frequency spectrum of the amplitude fluctuations is computed. Second, the theoretical spectrum is obtained by studying wave propagation in random media. Third, a turbulence model for the atmosphere is constructed by comparing the results from the first two steps. Finally, scintillation estimates for an entry probe link are estimated based on the turbulence model.

When the Pioneer 10 S-band radio occultation signals were processed it was found that there was strong scintillation produced by the Jovian ionosphere. Our attention has therefore been directed to the study of ionospheric rather than atmospheric scintillation. For the former, the fluctuations in refractive index are due to electron density irregularities in the ionosphere and a model for these irregularities will be constructed. The finding of Jovian ionospheric scintillation has important consequences for the radio design of future entry probes to Jupiter. The reason is that unlike the neutral atmosphere, the ionosphere is a dispersive medium and the scintillation increases when the radio frequency is lowered. Thus, the UHF

relay links that are being considered for the Jupiter entry probe missions may not be satisfactory for communications.

The analysis of the Pioneer 10 and 11 data has been considerably more difficult than that of Mariner 5 and so far we have interpreted but a small portion of the Pioneer 10 data. There are three reasons for this difficulty. First, in the upper part of the ionosphere the electron density irregularities appear to be anisotropic. This of course is not unusual since similar irregularities in the earth's ionosphere are known to be anisotropic due to alignment with the magnetic field. Second, since the ionosphere consists of many layers, multipath propagation effects are also present and these must be identified and distinguished from the scintillation effects. Finally, because of the large spacecraft-to-ionosphere distance and large extent of the ionosphere of Jupiter, the ionospheric scintillation is rather strong. In some regions of the ionosphere it is so strong that the variance σ_χ^2 of the log-amplitude fluctuations is close to one and the weak fluctuation theory is inadequate. Thus, anisotropy, multipath propagation and strong fluctuations are three new effects that must be studied and fully understood before the Pioneer 10 scintillations can be completely interpreted. Despite these problems considerable progress has been achieved and a preliminary model of the ionospheric irregularities that gives order-of-magnitude estimates of entry probe scintillation has been constructed.

II. Irregularity Model and Entry Probe Estimates

The background material for this report has been described in detail in Ref. 1 and will not be repeated. To understand the results discussed in this section the reader must read Ref. 1.

The latest information obtained on the Jovian electron density irregularities deduced from the Pioneer 10 radio occultation data is given in Ref. 3, which is reproduced in its entirety in the appendix of this report. Briefly, we found that the ionospheric irregularities existed over an altitude range of 3000 km on the late afternoon side probed by Pioneer 10 and over an altitude range of 2000 km in the early morning side. The structure constant c_n of the refractive index fluctuations characterizes the strength of the fluctuations. We have found that c_n lies in the range 3.3×10^{-9} to 4.9×10^{-9} $m^{-1/3}$ in the regions of ionosphere examined. The spatial wavenumber spectrum of the electron density irregularities is very close to the Kolmogorov spectrum and the outer scale size L_o is greater than 6 km.

The entry probe configuration is shown in Fig. 1. We will make scintillation estimates for a probe located at the zero altitude level, which corresponds to the level in the atmosphere of Jupiter where the refractivity is 10 (Refs. 3 and 4). The radial distance to this point on the late afternoon side is about 70435 km. We will assume that the irregularities extend to 3000 km and that $c_n = 5 \times 10^{-9}$ $m^{-1/3}$ and remains constant throughout this altitude range.

The raypath distance L through the ionospheric irregularities is an important parameter for estimating the scintillation of an entry probe. In terms of the communications angle θ, which is the angle the raypath makes with the zenith (see Fig. 1), L can be computed through the following relationships

$$\left.\begin{aligned} \theta_1 &= 180 - \theta \\ \theta_3 &= \sin^{-1}\left(\frac{L_3}{L_1}\sin\theta_1\right) \\ \theta_2 &= 180 - \theta_1 - \theta_3 \\ L &= L_1\,\frac{\sin\theta_2}{\sin\theta_1} \end{aligned}\right\} \qquad (1)$$

where θ, θ_1, θ_2 and θ_3 are in degrees. We have computed L for various values of θ and the results are shown in Table I.

The Fresnel size $\sqrt{\lambda L}$ corresponding to the $\theta = 90°$ case (L = 20775 km) is 1.646 km at S-band (2.3 GHz) and 3.95 km at 400 MHz. L_o is greater than these Fresnel sizes since from Pioneer 10 we have deduced that L_o exceeds 6 km. Under this condition and assuming the Kolmogorov spectrum, the variance σ_χ^2 of the log-amplitude fluctuations for the entry probe is (Ref. 1):

$$\sigma_\chi^2 = 0.308\, c_n^2\, k^{7/6}\, L^{11/6} \qquad (2)$$

where k is the free space wavenumber. Because of Fresnel filtering, scale sizes larger than $\sqrt{\lambda L}$ do not contribute to σ_χ^2. Consequently, (2) is independent of L_o. For the phase fluctuations, Fresnel filtering does not occur and the variance σ_ϕ^2 of phase fluctuations depends on L_o (Ref. 1):

$$\sigma_\phi^2 = 0.782\ k^2\ L_o^{5/3}\ c_n^2\ L - \sigma_\chi^2 \tag{3}$$

where σ_χ^2 is given by (2). It should be emphasized that (2) and (3) are only valid for weak fluctuations and the condition for weak fluctuations is that $\sigma_\chi^2 < 1$.

The refractive index n is $[1 - (\omega_p/\omega)^2]$ where ω_p is the plasma frequency and $\omega = kc$ (c is the speed of light). For $(\omega_p/\omega)^2 << 1$,

$$\sigma_n^2 \propto \frac{1}{4}\left(\frac{\omega_p}{\omega}\right)^4 \frac{\sigma_{n_e}^2}{n_e^2} \tag{4}$$

where n_e is the electron density, and σ_n^2 and $\sigma_{n_e}^2$ are the variances of the refractive index and electron density fluctuations, respectively. From the spatial wavenumber spectrum it can be shown that (Ref. 5)

$$c_n^2 \propto 1.9\ \sigma_n^2\ L_o^{-2/3} \tag{5}$$

It can be seen, therefore, that $c_n^2 \propto k^{-4}$.

The value of structure constant $c_n = 5 \times 10^{-9}\ m^{-1/3}$ derived from Pioneer 10 is for S-band only. For 400 MHz $c_n = 5 \times 10^{-9} \times F^2$ where $F = 2300/400$. We have computed σ_χ^2 and σ_ϕ^2 at S-band and 400 MHz for various values of θ. For the phase fluctuations we have made the calculations for two cases of L_o: 10 and 100 km. The results are summarized in Table II. σ_χ can be converted to the rms fluctuation in dB σ_{dB} by multiplying σ_χ by the factor $20/\ln 10 = 8.7$. As can be seen from Table II, although the amplitude fluctuations at S-band are small, they become substantial at 400 MHz. On the other hand, the phase fluctuations are large at both S-band and 400 MHz. It should be pointed out that even though the calculated results for σ_χ^2 at 400 MHz indicate that σ_χ^2 exceeds one for large θ, such values will not occur since σ_χ^2 saturates before reaching one (Ref. 6). When saturation occurs, (2) and (3), which are derived from weak fluctuation theory, are no longer valid and alternate results using strong fluctuation theory must be derived.

The frequency spectra of the log-amplitude and phase fluctuations [$W_\chi(f)$ and $W_S(f)$ respectively] indicate how the variance of the fluctuations is distributed in frequency. The bandwidth of the log-amplitude fluctuations f_{3dB} is given by (Ref. 1)

$$f_{3dB} = 0.294\ v_\perp \sqrt{\frac{k}{L}} \tag{6}$$

where $v_\perp$ is the wind velocity transverse to the line-of-sight path. Computed

values of f_{3dB} assuming $v_\perp$ = 100 m/sec are summarized in Table III and indicate that the spectrum is rather narrow.

The complete spectra of the log-amplitude and phase fluctuations are given in Ref. 1 (Figs. 3 and 4 in Ref. 1, respectively). These spectra are normalized with respect to $f_\perp$ and β which are

$$f_\perp = \frac{v_\perp}{2} \sqrt{\frac{k}{L}} \tag{7}$$

$$\beta = \frac{1}{L_o} \sqrt{\frac{L}{k}} \tag{8}$$

so that the spectra corresponding to the different specific cases can readily be obtained. It is interesting to note that the spectrum of the rather large phase fluctuations shown in Table II is also very narrow.

III. Earth's Ionosphere

In this section we would like to indicate some references in regards to scintillation in the earth's ionosphere. This would be helpful because the irregularities in the earth's ionosphere are similar and a large amount of scintillation measurements have been made. It must be emphasized that the literature on this subject is voluminous and we will mention just a few references.

A brief review of scintillation studies has recently been given by Hartmann (Ref. 7). The scintillation index S_4 is defined by

$$S_4 = \left[\langle A^4\rangle / \langle A^2\rangle^2 - 1\right]^{\frac{1}{2}} \tag{9}$$

where A is amplitude. When the amplitude fluctuations are small

$$S_4^2 \cong 4\,\sigma_\chi^2 \tag{10}$$

In the earth's ionosphere the variation of S_4 and consequently σ_χ^2 with zenith angle has been studied by Briggs and Parkin (Ref. 8). The variation of σ_χ^2 is due to the change in path length (discussed in the previous section) and change in the direction of wave propagation with respect to the magnetic field. The latter effect is due to the alignment of the irregularities with the magnetic field (anisotropy). The spatial wavenumber spectrum of electron density irregularities was assumed to be gaussian. Recent in situ (Ref. 9) as well as scintillation (Ref. 10) measurements indicate that the irregularity spectrum is power-law rather than gaussian. Rufenach has therefore repeated

the analysis of Briggs and Parkin using the power-law spectrum (Ref. 11). Scintillation depends on time of day and latitude. The global morphology of ionospheric scintillations has been discussed by Aarons *et al.* (Ref. 12), Crane (Ref. 13), Fremouw and Rino (Ref. 14) and Pope (Ref. 15). Most of the measurements made in the references listed above were carried out at UHF/VHF frequencies. Large S-band scintillations have recently been found in the equatorial region. These S-band scintillations are unexpected based on extrapolation of the UHF/VHF scintillations and this result has sparked several detailed studies of the frequency dependence of the scintillations (Refs. 16 and 17).

All the studies mentioned above were based on the scintillation index. The frequency spectrum has also been computed and studied by Elkins and Papagiannis (Ref. 18), Rufenach (Ref. 10), Singleton (Ref. 19) and Crane (Ref. 20). Crane's measurements are of particular interest since they were made at 400 MHz and include phase as well as amplitude fluctuations.

We have mentioned strong fluctuations and would like to point out that this represents an area of much active research (Refs. 21 and 22). Several excellent reviews of the current research have been published (Refs. 23-26).

Finally, a symposium on the effect of the ionosphere on space systems and communications was recently held and the proceedings contain many papers on current studies of scintillation and the ionospheric irregularities (Ref. 27).

IV. Conclusions and Future Work

We have obtained some estimates of scintillation for a Jovian entry probe. These estimates must be regarded as order-of-magnitude only since the irregularity model was constructed on the basis of the interpretation of just a portion of the Pioneer 10 data. To interpret the remaining data, the effects of anisotropy, multipath propagation and strong fluctuations must be analyzed. These effects may change the entry probe estimates significantly. As an example, it is felt that the structure constant c_n in the strong fluctuation region of the ionosphere is about a factor of 10 larger than that used in this report. Once the Pioneer 10 scintillation due to the ionosphere is completely interpreted, turbulence deep in the atmosphere of Jupiter can also be measured.

In this report we have included a short discussion of scintillation studies in the earth's ionosphere. The purpose is to indicate that scintillation depends on many factors and that even in the earth's ionosphere, which has been studied for many years, prediction is not straightforward. In fact, many aspects of ionospheric scintillation are still being actively investigated.

Table I

Summary of the Calculations of L in Terms of θ

θ (deg)	L (km)
0	3000
30°	3441
60°	5671
90°	20775

Table II

Summary of the Calculations for σ_χ^2 and σ_ϕ^2

θ (deg)	σ_χ^2		σ_ϕ^2 (rad^2) L_o = 10 km		σ_ϕ^2 (rad^2) L_o = 100 km	
	S-band	400 MHz	S-band	400 MHz	S-band	400 MHz
0	5.28×10^{-4}	7.65×10^{-2}	0.625	20.9	29	969.4
30	6.8×10^{-4}	9.84×10^{-2}	0.72	23.95	33.4	1111.9
60	1.7×10^{-3}	0.246	1.185	39.48	55	1832.5
90	1.83×10^{-2}	2.66	4.34	144.63	201.6	6713

Table III

Summary of f_{3dB} ($v_{\perp}$ = 100 m/sec)

θ (deg)	f_{3dB} at S-band (Hz)	f_{3dB} at 400 MHz (Hz)
0	0.117	0.05
30	0.11	0.05
60	0.085	0.036
90	0.045	0.019

References

1. Woo, R., Kendall, W., Ishimaru, A., and Berwin, R., "Effects of Turbulence in the Atmosphere of Venus on Pioneer Venus Radio - Phase I", Jet Propulsion Laboratory Technical Memorandum 33-644, June 30, 1973.

2. Woo, R., and Kendall, W., "Effects of Turbulence in the Atmosphere of Venus on Pioneer Venus Radio - Phase II", Jet Propulsion Laboratory Technical Memorandum 33-702, August 15, 1974.

3. Woo, R., and Yang, F. C., "Measurements of Electron Density Irregularities in the Ionosphere of Jupiter by Pioneer 10", paper presented at the Jupiter Conference held at the University of Arizona, May 18-22, 1975, and submitted for publication.

4. Fjeldbo, G., Kliore, A., Seidel, B., Sweetnam, D., and Cain, D., "The Pioneer 10 Radio Occultation Measurements of the Ionosphere of Jupiter", *Astron. Astrophys.*, 1975.

5. Strohbehn, J., "Line-of-Sight Wave Propagation Through the Turbulent Atmosphere", *Proc. IEEE*, Vol. 56, No. 8, pp. 1301-1318, August 1968.

6. Tatarski, V. I., "The Effects of the Turbulent Atmosphere on Wave Propagation", Nauka, Moscow, 1967, pg. 300. Translated and available from the U.S. Department of Commerce, Springfield, Va.

7. Hartmann, G. K., "Brief Review of Scintillation Studies", *Space Research XII*, Akademie-Verlag, Berlin, 1972, pp. 1221-1228.

8. Briggs, B. H., and Parkin, I. A., "On the Variation of Radio Star and Satellite Scintillations with Zenith Angle", *J. Atmos. Terr. Phys.*, Vol. 25, pp. 339-365, 1963.

9. Dyson, P. L., McClure, J. P., and Hanson, W. B., "In Situ Measurements of the Spectral Characteristics of F Region Ionospheric Irregularities", *J. Geophys. Res.*, Vol. 79, No. 10, pp. 1497-1502, April 1, 1974.

10. Rufenach, C. L., "Power-Law Wavenumber Spectrum Deduced from Ionospheric Scintillation Observations", *J. Geophys. Res.*, Vol. 77, No. 25, pp. 4761-4772, September 1, 1972.

11. Rufenach, C. L., "Ionospheric Scintillation by a Random Phase Screen: Spectral Approach", *Radio Science*, Vol. 10, No. 2, pp. 155-165, February 1975.

12. Aarons, J., Whitney, H. E., and Allen, R. S., "Global Morphology of Ionospheric Scintillations", *Proc. IEEE*, Vol. 59, No. 2, February 1971.

13. Crane, R. K., "Morphology of Ionospheric Scintillation", National Telecommunications Conference 1974 Record, IEEE Publ. 74 CHO 902-7 CSCB, pp. 285-290.

14. Fremouw, E. J., and Rino, C. L., "An Empirical Model for Average F-Layer Scintillation at VHF/UHF", *Radio Science*, Vol. 8, No. 3, pp. 213-222, March 1973.

15. Pope, J. H., "The Use of Global Ionospheric Irregularity Models for Satellite Communications", National Telecommunications Conference 1974 Record, IEEE Publ. 74 CHO 902-7 CSCB, pp. 292-295.

16. Rufenach, C. L., "Wavelength Dependence of Radio Scintillation: Ionosphere and Interplanetary Irregularities", *J. Geophys. Res.*, Vol. 79, No. 10, pp. 1562-1566, April 1, 1974.

17. Wernik, A. W., and Liu, C. H., "Ionospheric Irregularities Causing Scintillation at GHz Frequency Radio Signals", *J. Atmos. Terr. Phys.*, Vol. 36, pp. 871-879, 1974.

18. Elkins, T. J., and Papagiannis, M. D., "Measurement and Interpretation of Power Spectrums of Ionospheric Scintillation at a Sub-Auroral Location", *J. Geophys. Res.*, Vol. 74, No. 16, August 1, 1969.

19. Singleton, D. G., "Power Spectra of Ionospheric Scintillations", *J. Atmos. Terr. Phys.*, Vol. 36, pp. 113-133, 1974.

20. Crane, R. K., "Spectra of Amplitude and Phase Scintillation", Proceedings of the 1975 Symposium on the Effect of the Ionosphere on Space Sciences and Communications held at the Naval Research Laboratory, January 20-22, 1975.

21. Liu, C. H., Wernik, A. W., Yeh, K. C., and Youakim, M. Y., "Effects of Multiple Scattering on Scintillation of Transionospheric Radio Signals", *Radio Science*, Vol. 9, No. 6, pp. 599-607, June 1974.

22. Yeh, K. C., Liu, C. H., and Youakim, M. Y., "A Theoretical Study of the Ionospheric Scintillation Behavior Caused by Multiple Scattering", *Radio Science*, Vol. 10, No. 1, pp. 97-106, January 1975.

23. Barabanenkov, Yu. N., Kravstov, Yu. A., Rytov, S. M., and Tamarskii, V. I., "Status of the Theory of Propagation of Waves in a Randomly Inhomogeneous Medium", *Usp. Fiz. Nauk*, Vol. 102, pp. 3-42, September 1970. Translated in *Soviet Physics Uspekhi*, Vol. 13, No. 5, pp. 551-680, March-April 1971.

24. Prokhorov, A. M., Bunkin, F. V. Gochelashvily, K. S., and Shishov, V. I., "Laser Irradiance Propagation in Turbulent Media", *IEEE Proc.*, Vol. 63, No. 5, pp. 790-811, May 1975.

25. Gurvich, A. S., and Tatarskii, V. I., "Coherence and Intensity Fluctuations of Light in the Turbulent Atmosphere", *Radio Science*, Vol. 10, No. 1, pp. 3-14, January 1975.

26. Fante, R. L., "Propagation in Turbulent Media: A Review of Recent Progress", Air Force Cambridge Research Laboratories Report No. AFCRL-TR-75-0105, February 24, 1975.

27. Proceedings of the 1975 Symposium on the Effect of the Ionosphere on Space Systems and Communications sponsored by the Naval Research Laboratory, January 20-22, 1975, Arlington, Va.

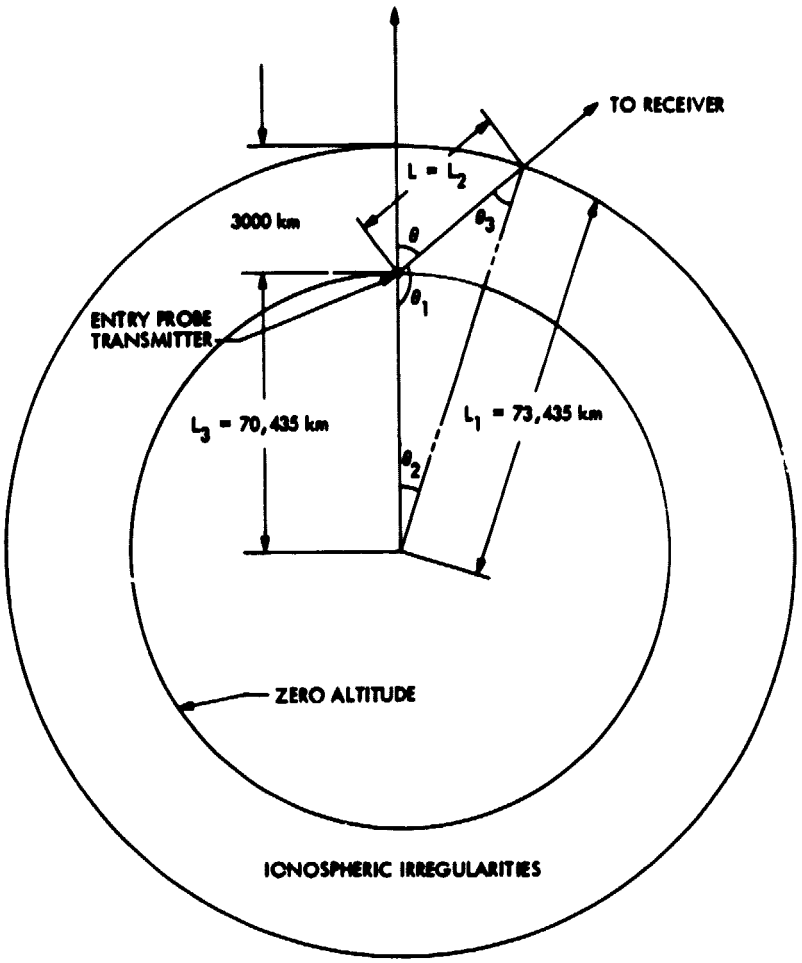

Fig. 1. Jupiter entry probe configuration

Appendix

Measurements of Electron Density Irregularities in the Ionosphere of Jupiter by Pioneer 10

(Presented at the Jupiter Conference held at the University of Arizona, May 18-22, 1975)

Abstract

In this paper we demonstrate that when the frequency spectrum of the log-amplitude fluctuations is used, the radio occultation experiment is a powerful tool for detecting, identifying and studying ionospheric irregularities.

Analysis of the Pioneer 10 radio occultation measurements reveals that the Jovian ionosphere possesses electron density irregularities which are very similar to those found in the earth's ionosphere. This is a significant result because it is the first time such irregularities have been found in a planetary ionosphere other than that of the earth. The Pioneer 10 results indicate that the spatial wavenumber spectrum of the electron density irregularities is close to the Kolmogorov spectrum and that the outer scale size is greater than the Fresnel size (6.15 km). This type of spectrum suggests irregularities produced by the turbulent dissipation of irregularities larger than the outer scale size.

I. Introduction

Many measurements of electron density irregularities in the earth's ionosphere have been made using ground-based and topside sounders, radio-star and satellite-beacon scintillations as well as in situ measurements. The total number of publications is very large but periodic reviews of the extensive literature have been made (Herman, 1966; Whitehead, 1970; Farley, 1973). Despite some progress in recent years, the production mechanisms are not all fully understood.

The Pioneer 10 S-band radio occultation experiment (Kliore *et al.*, 1974; Fjeldbo *et al.*, 1975) has provided the first measurements of the vertical electron density distribution in the Jovian ionosphere. During these measurements the radio signal underwent a significant amount of spectral broadening apparently due to ionospheric scintillations. In this paper we analyze these scintillations and show that they are caused by electron density irregularities similar to those found in the earth's ionosphere. This is an important result because it is the first time such irregularities have been found in a planetary ionosphere other than that of the earth.

A careful study of the Jovian ionospheric scintillations is important because any information obtained will contribute to our understanding of the formation of the electron density irregularities in the ionospheres of both Jupiter and the earth. There are practical reasons as well. First, the identification and estimates of the ionospheric scintillations will lead to improved accuracy in the electron density profiles derived from the radio occultation measurements. Second, the atmosphere of Jupiter

is expected to be turbulent and it would be highly desirable to detect and study the turbulence as has been done for Venus (Woo *et al.*, 1974; Woo, 1975). When the neutral atmosphere is being probed in the radio occultation experiment the ray path also traverses the ionosphere. The measured radio scintillations are therefore due to atmospheric turbulence as well as ionospheric irregularities, and to obtain measurements of turbulence one must first determine the ionospheric contribution. Third, a model of the ionospheric scintillations is urgently needed before the radio frequency of the communications link of future Jupiter entry probes can be selected. The reason is that UHF relay links are being seriously considered for future entry missions and ionospheric scintillation becomes more severe when the radio frequency is decreased.

Extensive information on the earth's ionospheric irregularities has been deduced from both radio-star and satellite scintillations. Much of the earlier work was based on the scintillation index (Briggs and Parkin, 1963; Aarons *et al.*, 1971; Wernik and Liu, 1974), which is a measure of the total power in the amplitude fluctuations. More recent work is based on the frequency spectrum of the amplitude fluctuations (Elkins and Papagiannis, 1969; Rufenach, 1972; Singleton, 1974), which indicates how the total power of the fluctuations is distributed in terms of the fluctuation frequency.

In principle, scintillation measurements made during radio occultation are similar to those made in the earth's ionosphere. However, there are major differences in terms of probing capabilities. Because of the generally long path length between the flyby spacecraft and the ionosphere

being probed, the scintillation is more severe. Thus, the radio occultation measurement is more sensitive and is ideal for detection purposes. Another important difference in the radio occultation measurement is that the line-of-sight path probes the top of the ionosphere first. As a result, it provides important information on vertical location, variation and extent of the ionospheric irregularities.

In this paper we will use the temporal frequency spectrum of the amplitude fluctuations to study the electron density irregularities. For radio occultation the time duration of the data is short and the signal-to-noise ratio generally low. In the case of Pioneer 10 the data were further affected by multipath propagation. For the radio occultation data it is therefore imperative to use the spectrum approach. From the standpoint of data processing the spectrum permits the separation of the scintillation, noise and multipath effects. From the standpoint of remote sensing the spectrum is very useful in deducing information on the strength and wavenumber spectrum of the electron density irregularities. In short, when the spectrum approach is used the radio occultation experiment is a powerful tool for detecting, identifying, locating and studying ionospheric irregularities.

This paper is organized in the following manner. The experimental results obtained from Pioneer 10 are given in Section II. The wave propagation theory is discussed in Section III. Information on the electron density irregularities is inferred in Section IV based on the comparison of the experimental and theoretical results. Finally, the conclusions are summarized in Section V.

II. Experimental Results

The Pioneer 10 radio occultation experiment has been described in detail by Kliore *et al.* (1974) and Fjeldbo *et al.* (1975). The electron density profiles derived by Fjeldbo *et al.* (1975) are reproduced in Figs. A-1, 2, 3. Altitude is referenced to the level in the lower neutral atmosphere that has a refractivity of 10. The late afternoon electron density profiles computed from the immersion data are shown in Figs. A-1 and A-2. The measurements were made at 26°N latitude and the solar zenith angle was approximately 81°. In Fig. A-1 the linear frequency drift term of the spacecraft's crystal oscillator was determined from the doppler residual data obtained in the 5500-10000 km altitude region. In Fig. A-2 a frequency drift rate change observed in the doppler residual data near 5300 km altitude was presumed caused by the spacecraft oscillator and the linear oscillator drift term was estimated by fitting a straight line to the doppler residual data obtained in the 4000 to 5300 km altitude region. Fig. A-3 is the early morning electron density profile computed from the emersion data. The measurements were made at 58°N latitude and the solar zenith angle was about 95°. The linear oscillator frequency drift was removed by fitting a straight line to the doppler residual data obtained in the 5500-10000 km altitude range.

Our analysis of the electron density irregularities is based on the temporal frequency spectrum $W_\chi(f)$ of the log-amplitude fluctuations, which is computed in the following manner. The time history of amplitude is obtained by summing the squares of the phase quadrature components of the received signal and then taking the square root. After conversion to

log-amplitude, a constant bias is subtracted so that the mean of the log-amplitude fluctuations is zero. The resulting time history of the log-amplitude fluctuations has a minimum sampling rate of 500 samples per second and is spectrum analyzed using an FFT algorithm described previously (Woo *et al.*, 1974).

We have examined three altitude ranges for both the immersion and emersion data. The three regions for each set of data are indicated in Figs. A-1, 2, 3 and are denoted A, B and C. The corresponding frequency spectra of the S-band log-amplitude fluctuations are shown in Figs. A-4 through A-9. The regions other than A, B and C will not be discussed in this paper because the theory which will be described in Section III is inadequate for interpreting the spectra. The solid curves in Figs. A-5, 6, 8 and 9 represent the computed spectra while the dashed curves are the theoretical spectra which will be discussed in Section III. The 90% confidence intervals for the spectra are also indicated. The spectra of both the immersion and emersion data for region A are approximately flat and essentially represent the system noise. As can be seen in Figs. A-4 and A-7 the noise spectral density level is approximately 10^{-3}. This is close to the value which would be expected when the SNR (signal-to-noise ratio) in a 1 Hz bandwidth is 30 dB, since the noise spectral density level for the log-amplitude fluctuations is approximately 1/SNR.

The spectra for regions B and C clearly show structure for fluctuation frequencies below approximately 10 Hz. Above 10 Hz, the spectra are essentially those of the system noise. The low-frequency structure is present in all the immersion data below 3000 km and in all the emersion data below

2000 km. It should be pointed out that the spectra for regions B and C cover very short periods of time. However, because the spectra are rather wide (10 Hz), good definition of the spectrum shape is still achieved.

III. Theory

We have seen in the previous section that the frequency spectrum is very useful when analyzing fluctuations in the data since the structure and noise components can be separated in the frequency domain. Our next step is to derive the theoretical spectrum for scintillation so that scintillation can be identified and information on the electron density irregularities can be deduced from the measurements.

We will use the results obtained previously for atmospheric turbulence (Woo and Ishimaru, 1974) to derive the theoretical spectrum for ionospheric scintillation. The only change that need be made for ionospheric scintillation is to relate the electron density and refractive index fluctuations and we will do this in Section IV.

The radio occultation geometry is shown in Fig. A-10. The x-axis is the line-of-sight path and L is the distance between the spacecraft and the Jovian ionosphere. We will assume that the region of ionospheric irregularities being probed can be approximated by an ellipsoid (see Fig. A-11). The structure constant c_n of the refractive index fluctuations is then given by

$$c_n^2 = c_{no}^2 \exp\left[-\left(\frac{x-L}{a}\right)^2 - \left(\frac{y}{b}\right)^2 - \left(\frac{z}{a}\right)^2\right] \qquad \text{(A-1)}$$

where c_{no} is the peak structure constant, a is the extent of the irregularities in the x-z plane and b is the extent in the y direction. a and b are related to each other by the following approximate relationships

$$a = H \tan\theta \tag{A-2}$$

$$\theta = \cos^{-1}\left(\frac{H}{H+b}\right) \tag{A-3}$$

where H is defined in Figs. A-10 and A-11.

In the earth's ionosphere recent scintillation (Elkins and Papagiannis, 1969; Rufenach, 1972; Singleton, 1974) and in situ (Dyson *et al.*, 1974) measurements of the electron density irregularities indicate that the spatial wavenumber spectrum $\Phi_n(\kappa)$ of the irregularities follows approximately a power law:

$$\Phi_n(\kappa) = \left(\kappa^2 + \frac{1}{L_o^2}\right)^{-p/2} \tag{A-4}$$

where κ is the spatial wavenumber, p is the spectral index and L_o is the outer scale size. In the earth's ionosphere the range of the spectral index is 3.4-5 and L_o is at least several kilometers. We will assume that the spatial wavenumber spectrum for the electron density irregularities in the Jovian ionosphere is also power-law and given by (A-4).

The size of the first Fresnel zone, hereafter called Fresnel size, is of the order of $\sqrt{\lambda L}$, where λ is the wavelength of the radio frequency and L is defined in Figs. A-10 and A-11. In the case of Pioneer 10 the Fresnel size is approximately 6.15 km. Since the ionosphere of Jupiter is much more extensive than that of the earth it is reasonable that L_o is

correspondingly larger too. We will assume that for Pioneer 10 $L_o > \sqrt{\lambda L}$. Furthermore, it is also clear that $a >> \sqrt{\lambda L}$ and $b >> \sqrt{\lambda L}$. Using these approximations and the spectrum given in (A-5), it can easily be shown following Woo and Ishimaru (1974) that

$$W_\chi(f) = 0.033\, c_{no}^2\, 8\pi^2 k^2\, \frac{\pi a}{2v}\left(\frac{\omega^2}{v^2} + \frac{1}{L_o^2}\right)^{(1-p)/2} \cdot \left\{ \psi\left[\frac{1}{2}, \frac{3-p}{2}; \frac{L^2}{k^2 a^2}\left(\frac{\omega^2}{v^2} + \frac{1}{L_o^2}\right)\right] - \mathrm{Re}\left\{ \exp\left[i\,\frac{L}{k}\,\frac{\omega^2}{v^2} - \frac{1}{4}\left(\frac{a\omega^2}{kv^2}\right)^2\right] \cdot \psi\left[\frac{1}{2}, \frac{3-p}{2}; -i\,\frac{L}{k}\left(\frac{\omega^2}{v^2} + \frac{1}{L_o^2}\right)\right]\right\}\right\} \qquad \text{(A-5)}$$

where $W_\chi(f)$ is the frequency spectrum of the log-amplitude fluctuations, k is the free space wavenumber, v is the velocity of the line-of-sight path transverse to the line-of-sight path, $\omega = 2\pi f$, f is the fluctuation frequency, Re{ } means real part of { }, and $\psi(a, c; z)$ is the confluent hypergeometric function (Abramowitz and Stegun, 1964), which is independent of the Kummer function ${}_1F_1(a, c; z)$. A number of important points in regards to the derivation of (A-5) are worth emphasizing. First, a three-dimensional model rather than the more common phase-screen approximation was used to represent the ionospheric scintillation. Second, Rytov's method was employed and this is valid only for weak fluctuations. The condition for weak fluctuations is that the variance σ_χ^2 of log-amplitude fluctuations be less than one. The variances for the respective spectra have been computed for fluctuation frequencies up to 10 Hz. The results are given in Table 1 and as can be seen the highest value for σ_χ^2 is 0.31.

Thus, weak fluctuation theory is applicable (Tatarski, 1971).

The theoretical spectrum given in (A-5) has the following input parameters: structure constant c_{no}, spectral index p, transverse velocity of the line-of-sight path v, distance between the spacecraft and the ionosphere L, free space wavenumber k, extent of the region of irregularities in the horizontal plane a, and the outer scale size L_o. v and L are known from the trajectory and k from the radio link. a can be estimated from knowledge of the vertical extent of the region of irregularities. Since a is greater than the Fresnel size it is not surprising that the spectrum shape shows no dependence on a in the range of values estimated. As discussed earlier we assume that L_o is greater than the Fresnel size. Under this condition the spectrum is independent of L_o since scale sizes larger than the Fresnel size do not contribute to the spectrum on account of Fresnel filtering (Tatarski, 1971). It is clear that there are only two unknowns: c_{no} and p. Examination of (A-5) reveals that c_{no} controls the level and not the shape of the spectrum. Thus, the only parameter that controls the shape of the spectrum is p.

We have computed the theoretical spectra by numerical integration of the confluent hypergeometric function. Shown in Fig. A-12 are the results for a given set of values for v, L, a, k and L_o and three cases of p. The spectra are normalized to their values at $f = 10^{-1}$ Hz. The p = 11/3 case is of special interest because it corresponds to the Kolmogorov spectrum which has physical basis and lies within the spectral index range observed in the earth's ionosphere. As expected the shape of the spectrum is sensitive to the spectral index p. We can obtain the asymptotic expression

for the high frequency portion of the spectrum by using the appropriate asymptotic forms for $\psi(a, c; z)$. We get

$$W_\chi(f) \underset{f \to \infty}{=} 0.033\, c_{no}^2\, 8\pi^2\, k^2\, \frac{\pi a}{2v}\, \frac{\Gamma\left(\frac{p-1}{2}\right)}{\Gamma\left(\frac{p+1}{2}\right)} \left(\frac{\omega^2}{v^2}\right)^{(1-p)/2} \tag{A-6}$$

where Γ is the gamma function. Thus, it can be seen that when the frequency spectrum $W_\chi(f)$ is plotted on a log-log scale, the slope is (1-p) in the high fluctuation frequency region.

IV. Discussion

Let us now compare the theoretical and experimental spectra. v is approximately 35 km/sec, L is 2.2×10^5 km for immersion and 2.9×10^5 km for emersion and k is 48 m^{-1}. As discussed in the previous section the spectrum does not depend on L_o as long as L_o is larger than the Fresnel size or on a for the expected range of values. For the theoretical spectra we have assumed L_o = 100 km and a = 10000 km. The theoretical spectra in Figs. 5, 6, 8 and 9 correspond to p = 11/3 (Kolmogorov spectrum). The good agreement between the theoretical and experimental spectra indicates that the spatial wavenumber spectrum of the electron density irregularities is close to the Kolmogorov spectrum. Furthermore, the agreement justifies the weak fluctuation theory since the measured spectra would be broader for strong fluctuations (Gurvich and Tatarski, 1975).

The finding that the spatial wavenumber spectrum of the irregularities is close to Kolmogorov suggests that initially the irregularities are generated at L_o or at scale sizes greater than L_o and that the dissipation of the energy associated with these irregularities occurs by generating smaller and smaller irregularities. The highest fluctuation frequency measured is about 10 Hz. Since the velocity of the line-of-sight path is 35 km/sec, the smallest scale size measured is approximately 35/10 = 3.5 km. To measure smaller scale sizes the SNR must be increased.

The low frequency asymptotic expression of $W_\chi(f)$ for the Kolmogorov spectrum can be obtained:

$$W_\chi(f) \underset{f \to 0}{=} 0.033\, c_{no}^2\, \pi^{5/2}\, \frac{k^{2/3}\, a}{v}\, L^{4/3}\, \frac{27}{4}\, \Gamma\left(\frac{5}{3}\right) \tag{A-7}$$

Also, from (6) we have

$$W_\chi(f) \underset{f \to \infty}{=} 0.033\, c_{no}^2\, 8\pi^2\, k^2\, \frac{\pi a}{2v}\, \frac{\Gamma\left(\frac{4}{3}\right)}{\Gamma\left(\frac{11}{6}\right)}\, \left(\frac{\omega^2}{v^2}\right)^{-4/3} \tag{A-8}$$

The intersection of (A-7) and (A-8) defines the approximate frequency at which the "knee" of the spectrum W_χ is located. If we call this frequency f_k, we get

$$f_k = 0.414\, \frac{v}{\sqrt{\lambda L}} \tag{A-9}$$

f_k essentially defines the fluctuation frequency at which Fresnel filtering takes effect. As expected the scale size corresponding to f_k is approximately the Fresnel size. It is interesting to note that the spectrum is broader the higher the velocity, the higher the radio frequency or the closer the spacecraft is to the planet.

Another point worth mentioning is that the evidence of Fresnel filtering in the measured spectrum is the most prominent feature for identifying scintillation. It is obvious that the fluctuations in the amplitude of the signal could also be caused by the radio ray cutting through stratified layers of electron density in the ionosphere. However, if this were the case, there is no reason for the spectrum of such fluctuations to exhibit the effects of Fresnel filtering.

The next parameter we wish to estimate is c_{no} and this can be obtained either from the spectrum using (A-7) or from the variance σ_χ^2. If we assume the Kolmogorov spectrum along with the approximations used in the derivation of the frequency spectrum given in (A-5) we obtain following Woo and Ishimaru (1974):

$$\sigma_\chi^2 \simeq c_{no}^2 \; k^{7/6} \; L^{5/6} \; a \qquad \text{(A-10)}$$

When $\sigma_\chi^2 << 1$, $\sigma_\chi^2 \simeq m^2/4$, where m is the scintillation index. To estimate a we use (A-2) and (A-3) and make the following assumptions: (1) the radial distance to zero altitude is 70435 and 67980 km on the immersion and emersion sides respectively, and (2) the irregularities on the immersion

and emersion sides extend to 3000 and 2000 km respectively. The results of the estimates for c_{no} and a obtained from $W_\chi(0)$ are summarized in Table A-I.

It must be emphasized that (1) is a highly simplified model of the spatial variation of the structure constant c_n. In effect (1) simply defines the extent of the irregularities. Although the choice of (1) is not critical as far as the shape of the frequency spectrum W_χ is concerned, it is certainly important when seeking information on the variation of c_n with altitude. Thus, although the estimates of c_{no} given in Table A-I are crude they nevertheless indicate order of magnitude as well as relative magnitude.

Let us now relate the structure constant c_{no} of the refractive index fluctuations to the electron density fluctuations. Since the refractive index n is $[1 - (\omega_p/\omega)^2]^{\frac{1}{2}}$ where ω_p is the plasma frequency, we obtain for $(\omega_p/\omega)^2 << 1$

$$\sigma_n^2 \simeq \frac{1}{4}\left(\frac{\omega_p}{\omega}\right)^4 \frac{\sigma_{n_e}^2}{n_e^2} \tag{A-11}$$

where n_e is the electron density, and σ_n^2 and $\sigma_{n_e}^2$ are the variances of the refractive index and electron density fluctuations respectively. From the spatial wavenumber spectrum of the refractive index fluctuations it can be shown (Strohbehn, 1968) that

$$c_{no}^2 \simeq 1.9\ \sigma_n^2\ L_o^{-2/3} \tag{A-12}$$

so that

$$\frac{\sigma_{n_e}}{n_e} \propto 1.45 \left(\frac{\omega}{\omega_p}\right)^2 c_{no} L_o^{1/3} \qquad \text{(A-13)}$$

We have applied (A-13) to region B of both the immersion and emersion data and the results are summarized in Table A-II. As can be seen the fluctuations in electron density are substantial particularly on the emersion side which was probed during the early morning. However, the values of σ_{n_e}/n_e do not appear too different from those measured in the earth's ionosphere (Dyson *et al.*, 1974). The electron density profiles in Figs. A-1, 2, 3 exhibit a "wiggly" structure in region B. It is now clear that such structure is most likely not real and probably represents the effect of the electron density irregularities. In fact the percentage of the wiggles in terms of the average electron density is highest in Fig. A-2 and lowest in Fig. A-1 which is in agreement with the results summarized in Table A-II. In this regard, it is also clear from the results for region C that the layers L_6 and L_7 are most likely due to electron density irregularities. This conclusion is supported by the absence of distinct signatures of layers for L_6 and L_7 found by Fjeldbo *et al.* (1975).

V. Conclusion

We have demonstrated that when the frequency spectrum of the log-amplitude fluctuations is used, the radio occultation experiment is a powerful tool for detecting, identifying and studying ionospheric irregularities.

Analysis of the Pioneer 10 radio occultation measurements reveals that the Jovian ionosphere possesses electron density irregularities which are very similar to those found in the earth's ionosphere. This is a significant result because it is the first time such irregularities have been found in a planetary ionosphere other than that of the earth. The Pioneer 10 results indicate that the spatial wavenumber spectrum of the electron density irregularities is close to the Kolmogorov spectrum and that the outer scale size is greater than the Fresnel size (6.15 km). This type of spectrum suggests irregularities produced by the turbulent dissipation of irregularities larger than the outer scale size.

We have examined only a portion of the Pioneer 10 data in this paper. The remaining data indicate the presence of anisotropy in the irregularities as well as strong fluctuations. Analysis of this latter data is not complete and the results will be discussed in a later publication.

In the case of the earth's ionosphere, the electron density irregularities depend on latitude, time, season, sunspot number, magnetic field orientation, etc. Future radio occultation measurements are important in order to determine the dependence of the irregularities on these factors in the Jovian ionosphere. This information will contribute to our understanding of the formation of the irregularities not only in the Jovian ionosphere but the earth's ionosphere as well.

Acknowledgements

We thank the Pioneer 10 S-band Radio Occultation Team for their permission to analyze the Pioneer 10 data. The results presented in this paper were only possible through their efforts in making the Pioneer 10 radio occultation experiment a successful one. We are grateful to G. Fjeldbo and A. Kliore for numerous discussions in regard to the radio occultation experiment, W. Kendall fo. assistance in data processing, and C. Stelzried and G. Levy for support throughout the course of this work.

References

AARONS, J., WHITNEY, H. E., AND ALLEN, R. S. (1971). Global morphology of ionospheric scintillations. *Proc. IEEE* 59, 159.

ABRAMOWITZ, M., AND STEGUN, I. S., Eds. (1964). *Handbook of Mathematical Functions*. NBS Appl. Math. Ser. No. 55, Wash., D.C. 503

BRIGGS, B. H., AND PARKIN, I. A. (1963). On the variation of radio star and satellite scintillations with zenith angle. *J. Atmos. Terr. Phys.* 25, 339.

DYSON, P. L., MC CLURE, J. P., AND HANSON, W. B. (1974). In situ measurements of the spectral characteristics of F region ionospheric irregularities. *J. Geophys. Res.* 79, 1497.

ELKINS, T. J., AND PAPAGIANNIS, M. D. (1969). Measurement and interpretation of power spectrums of ionospheric scintillation at a sub-auroral location. *J. Geophys. Res.* 74, 4105.

FARLEY, D. T. (1974). Irregularities in the equatorial ionosphere: The Berkner symposium. *Rev. Geophys. Sp. Phys.* 12, 285.

FJELDBO, G., KLIORE, A., SEIDEL, B., SWEETNAM, D., AND CAIN, D. (1975). The Pioneer 10 radio occultation measurements of the ionosphere of Jupiter. *Astron. Astrophys.*

GURVICH, A. S., AND TATARSKI, V. I. (1975). Coherence and intensity fluctuations of light in the turbulent atmosphere. *Rad. Sci.* 10, 3.

HERMAN, J. R. (1966). Spread F and ionospheric F-region irregularities. *Rev. Geophys.* 4, 255.

KLIORE, A., CAIN, D. L., FJELDBO, G., SEIDEL, B. L. AND RASOOL, S. I. (1974). Preliminary results on the atmospheres of Io and Jupiter from the Pioneer 10 S-band occultation experiment. *Science*, 183, 323.

RUFENACH, C. L. (1972). Power-law wavenumber spectrum deduced from ionospheric scintillation observations. *J. Geophys. Res.* 77, 4761.

SINGLETON, D. G. (1974). Power spectra of ionospheric scintillations. *J. Atmos. Terr. Phys.* 36, 113.

STROHBEHN, J. W. (1968). Line-of-sight wave propagation through the turbulent atmosphere. *Proc. IEEE* 56, 1301.

TATARSKI, V. I. (1971). *The Effects of the Turbulent Atmosphere on Wave Propagation.* National Technical Information Service, 472 pp.

WERNIK, A. W., AND LIU, C. H. (1974). Ionospheric irregularities causing scintillation of GHz frequency radio signals. *J. Atmos. Terr. Phys.* 36, 871.

WHITEHEAD, J. D. (1970). Production and prediction of sporadic E. *Rev. Geophys. Sp. Sci.* 8, 65.

WOO, R. (1975). Observations of turbulence in the atmosphere of Venus using Mariner 10 radio occultation measurements. *J. Atmos. Sci.* 32, 1084.

WOO, R., AND ISHIMARU, A. (1974). Effects of turbulence in a planetary atmosphere on radio occultation. *IEEE Trans. Ant. Prop.* 22, 566.

WOO, R., ISHIMARU, A., AND KENDALL, W. B. (1974). Observations of small-scale turbulence in the atmosphere of Venus by Mariner 5. *J. Atmos. Sci.* 31, 1698.

TABLE A-I

SUMMARY OF MEASURED AND INPUT PARAMETERS

Region	σ_χ^2	H(km)	b(km)	θ(rad)	a(km)	$W_\chi(0)(Hz^{-1})$	$c_{no}(m^{-1/3})$
B of Immersion	0.24	71435	2000	0.234	17022	6×10^{-2}	4.47×10^{-9}
C of Immersion	0.22	70661	2774	0.276	19993	4.3×10^{-2}	3.49×10^{-9}
B of Emersion	0.105	69480	500	0.12	8350	2.3×10^{-2}	3.287×10^{-9}
C of Emersion	0.31	68240	1740	0.223	15508	6.8×10^{-2}	4.147×10^{-9}

TABLE A-II

SUMMARY OF σ_{n_e}/n_e

Region	n_e (electrons/cc)	ω_p/ω	σ_{n_e}/n_e (%)	
			L = 10 km	L = 100 km
Region B Immersion using n_e profile in Fig. 1	10^5	1.238×10^{-3}	9.11	19.63
Region B Immersion using n_e profile in Fig. 2	5×10^4	8.75×10^{-4}	18.24	39.3
Region B Emersion	2×10^4	5.54×10^{-4}	33.5	72.0

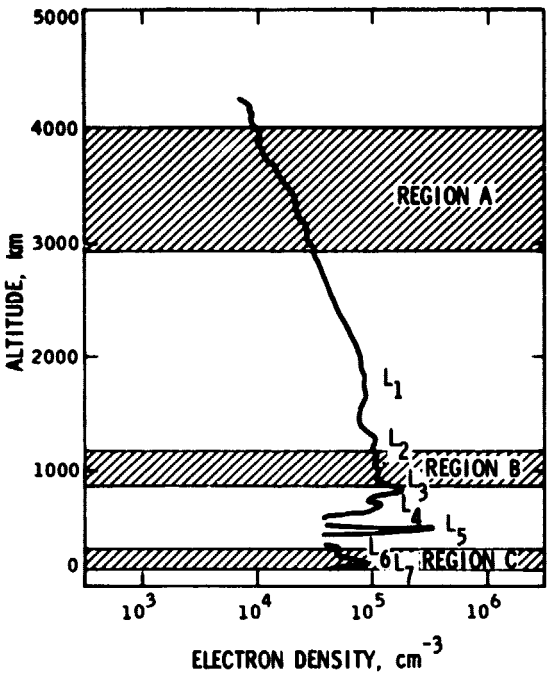

Fig. A-1. Late afternoon electron density profile derived from the immersion data by Fjeldbo et al. (1975). Frequency spectra of the log-amplitude fluctuations for regions A, B, and C are shown in Figs. A-4, 5, 6.

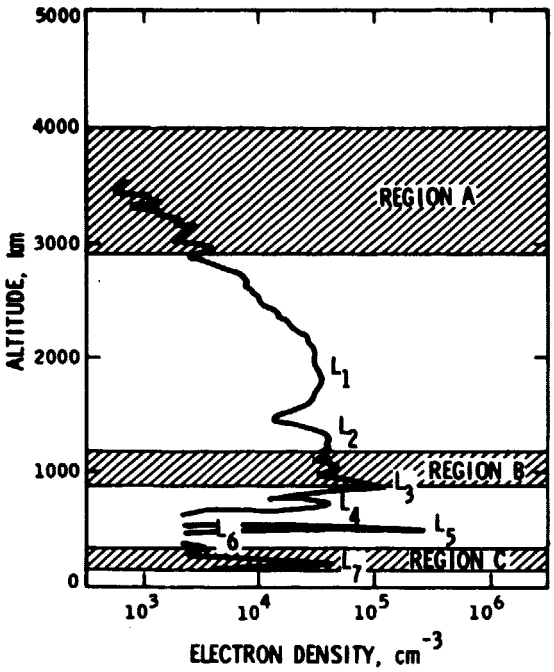

Fig. A-2. Late afternoon electron density profile derived from the immersion data by Fjeldbo et al. (1975). See text for difference from Fig. A-1. Frequency spectra of the log-amplitude fluctuations for regions A, B, and C are shown in Figs. A-4, 5, 6.

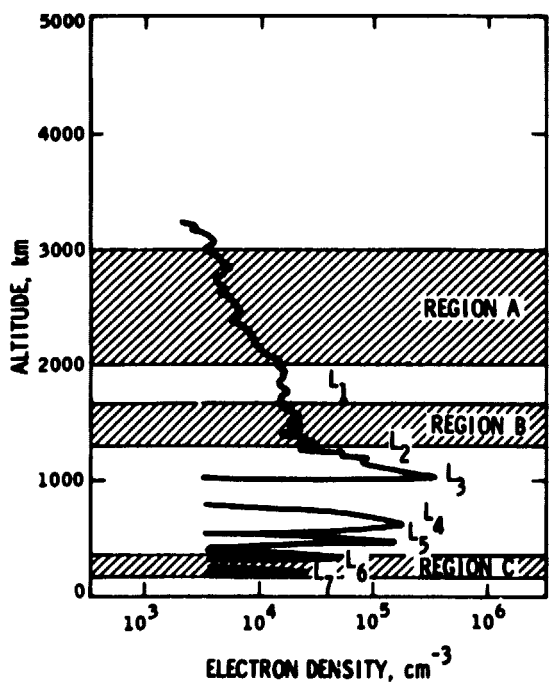

Fig. A-3. Early morning electron density profile derived from the emersion data by Fjeldbo et al. (1975). Frequency spectra of the log-amplitude fluctuations for regions A, B, and C are shown in Figs. A-7, 8, 9.

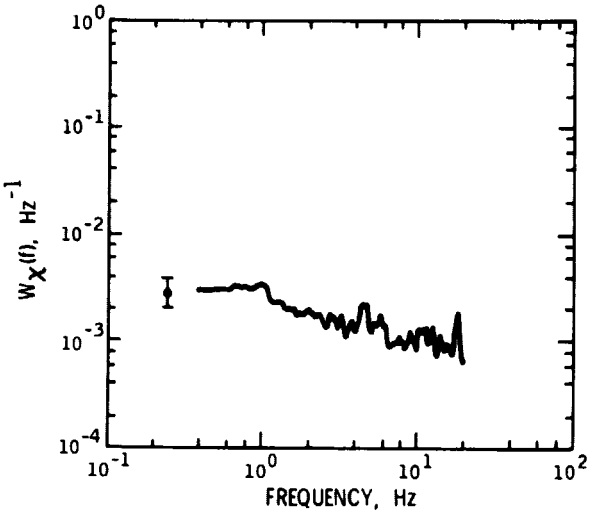

Fig. A-4. Frequency spectrum of the log-amplitude fluctuations for region A of immersion.

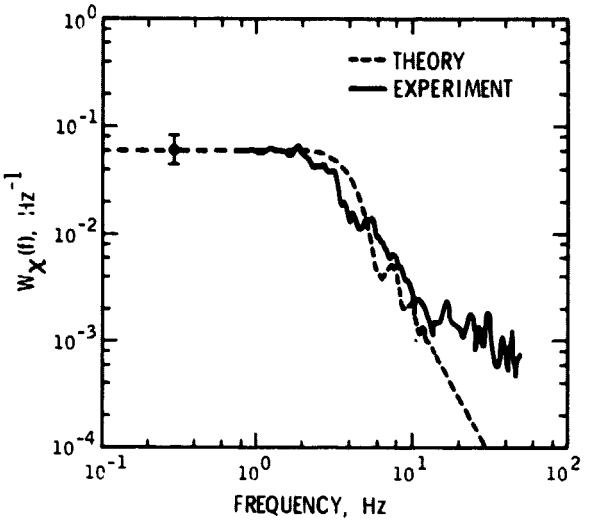

Fig. A-5. Frequency spectrum of the log-amplitude fluctuations for region B of immersion. For the theoretical spectrum, $p = 11/3$, $v = 35$ km/sec, $L = 2.2 \times 10^5$ km, $k = 48$ m^{-1}, $a = 10^4$ km and $L_o = 100$ km.

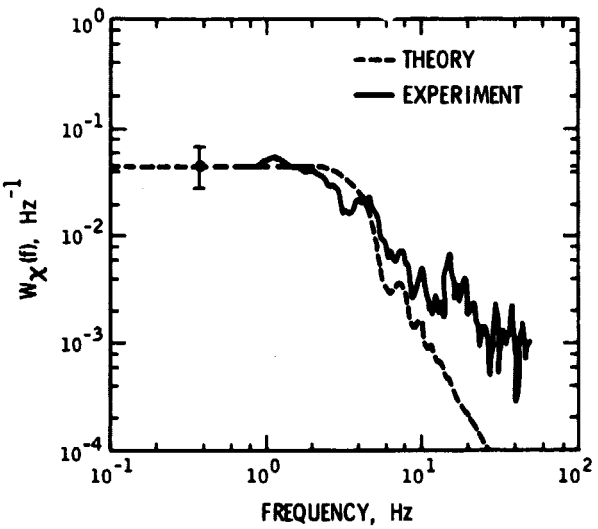

Fig. A-6. Frequency spectrum of the log-amplitude fluctuations for region C of immersion. For the theoretical spectrum, the parameters are the same as those used in Fig. A-5.

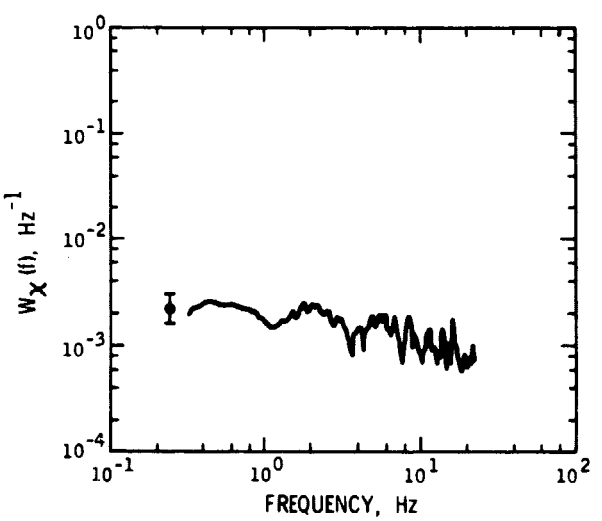

Fig. A-7. Frequency spectrum of the log-amplitude fluctuations for region A of emersion.

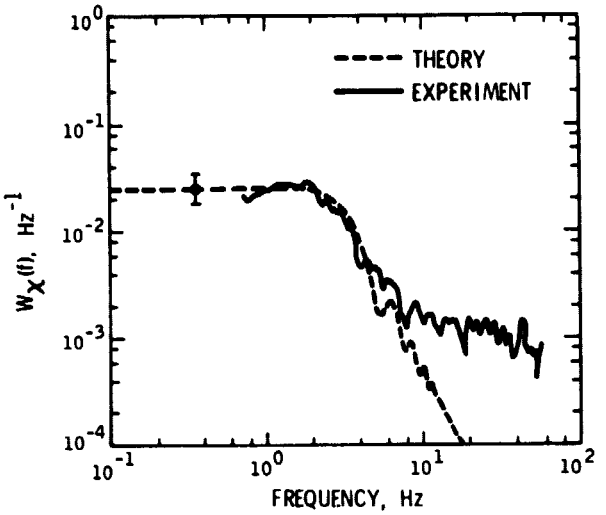

Fig. A-8. Frequency spectrum of the log-amplitude fluctuations for region B of emersion. For the theoretical spectrum, p = 11/3, v = 35 km/sec, L = 2.9 x 10^5 km, k = 48 m^{-1}, a = 10^4 km and L_o = 100 km.

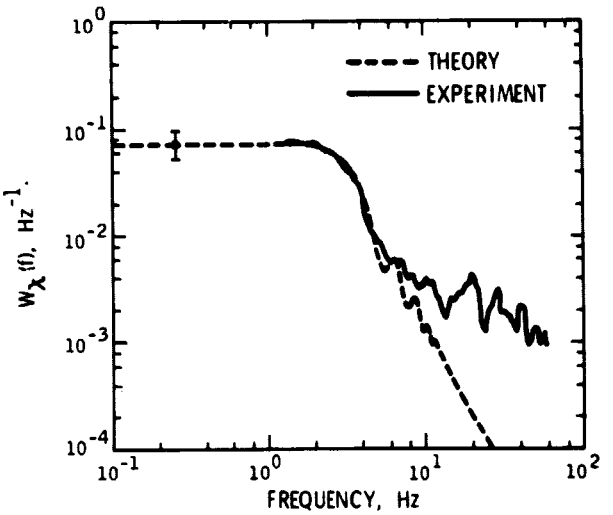

Fig. A-9. Frequency spectrum of the log-amplitude fluctuations for region C of emersion. For the theoretical spectrum, the parameters are the same as those used in Fig. A-8.

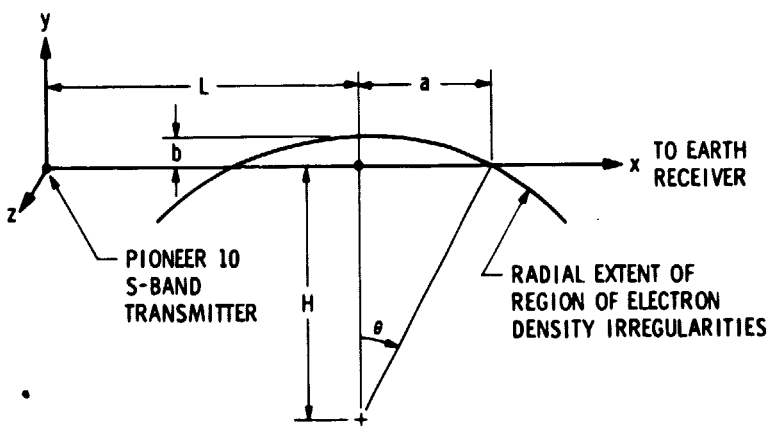

Fig. A-10. Radio occultation configuration.

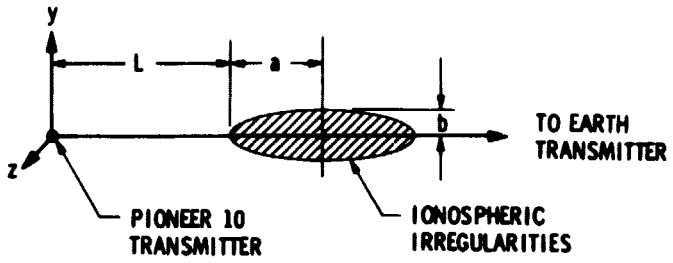

Fig. A-11. Ellipsoidal representation of the region of ionospheric irregularities.

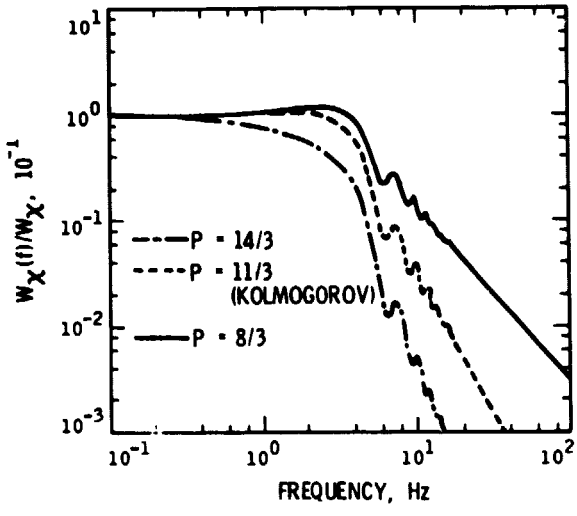

Fig. A-12. Frequency spectrum of the log-amplitude fluctuations for various values of p. v = 35 km/sec, L = 2.2 x 10^5 km, k = 48 m^{-1}, a = 10^4 km, and L_o = 100 km.

NASA—JPL—Comi., L.A., Calif.